JOURNAL OF SOLID STATE CHEMISTRY 39, 277–287 (1981)

Origin of the Yellow Color of Complex Nickel Oxides

GEORGE R. ROSSMAN

Division of Geological and Planetary Sciences, California Institute of Technology, Pasadena, California 91125*

AND ROBERT D. SHANNON AND ROBERT K. WARING

Central Research and Development Department,† E. I. du Pont de Nemours & Co., Wilmington, Delaware 19898

Received January 30, 1981; in revised form April 20, 1981

Single-crystal optical absorption spectra of NiO, $NiTiO_3$, $NiWO_4$, NiV_2O_6, $NiNb_2O_6$, Ni_2SiO_4, $Ni_3V_2O_8$, $LiNiPO_4$, $Li_2Ni_2Mo_3O_{12}$, $SrNiTeO_6$, $LiScSiO_4$:Ni, $MgSiO_3$:Ni, and $(Mg,Ni)_2SiO_4$ are presented for the purpose of comparing the spectra of yellow and green Ni^{2+} compounds. Powder spectra of $NiTiO_3$, $NiWO_4$, NiV_2O_6, $NiNb_2O_6$, and $Ni_3V_2O_8$ in the ultraviolet region help elucidate the more intense charge transfer bands. Bright yellow color results when Ni^{2+} is in a six-coordinated site significantly distorted from octahedral symmetry. Increased absorption intensity occurs when the metal ion *d–d* bands are in proximity to an ultraviolet charge transfer band.

Introduction

Ni^{2+} in sixfold coordination in oxides generally produces green colors. After observing that Ni^{2+} is bright yellow in the distorted $M(2)$ site of $LiNiPO_4$ of the olivine structure and in orthopyroxenes, where it apparently is in the large and distorted $M(2)$ site, we initiated a study of Ni^{2+} in a variety of compounds to determine if the size of the Ni^{2+} site, its distortion, or other factors were responsible for yellow nickel compounds. Materials examined included those with Ni^{2+} in mineral structures, (three olivines and one pyroxene), and the synthetic compounds $NiTiO_3$, $LiNiPO_4$, $NiWO_4$, $NiNb_2O_6$, Sr_2NiTeO_6, $Li_2Ni_2Mo_3O_{12}$, $Ni_3V_2O_8$, and NiV_2O_6. Emphasis was placed on single-crystal measurements which recovered both spectroscopic anisotropy and the absolute intensity of absorption and on powder reflectance measurements which allowed intensity measurements in the highly absorbing uv region between 260 and 450 nm.

Experimental Details

The olivines Ni_2SiO_4, $(Mg,Ni)_2SiO_4$, and $LiScSiO_4$:Ni, and the orthopyroxene $MgSiO_3$:Ni were grown by Jun Ito from a lithium molybdate–vanadate melt (*1, 2*). Electron microprobe analyses showed the following components by weight percent: $(Mg,Ni)_2SiO_4$: NiO, 46.06; FeO, 0.06; Al_2O_3, 0.12; V_2O_3, 0.49; $LiScSiO_4$:Ni: NiO, 7.03; V_2O_3, 0.08; FeO, 0.03; $MgSiO_3$:Ni: NiO, 4.18. NiO in the form of emerald green octahedra was grown from a

* Contribution No. 3532.
† Contribution No. 2875.

0022-4596/81/120277-11$02.00/0

concentrated KOH solution in a gold tube at 700°C and 3000 atm. Dark red crystals of $NiTiO_3$ were grown from a Pb-vanadate flux as described by Garton *et al.* (*3*). The larger crystals contain flux inclusions of an unidentified nature. An emission spectroscopic analysis showed the major impurities to be V, 0.2–1%; Fe, 0.1–0.5%; and Pb, <500 ppm. We feel the good agreement between the powder diffuse reflectance data and single-crystal absorption data eliminates the possibility that the major absorption peaks have these impurities as their origin. Yellow-orange $LiNiPO_4$ crystals were grown by the method of Zambonini and Malossi (*4*). Yellow-brown crystals of $Ni_3V_2O_8$ were grown from a KVO_3 flux. Brown crystals of $NiWO_4$ were grown from a Na_2WO_4 flux according to the method of Wanklyn (*5*). Yellow crystals of $NiNb_2O_6$ and yellow-brown crystals of $Li_2Ni_2Mo_3O_{12}$ were grown according to Wanklyn *et al.* (*6*). Yellow-brown crystals of Sr_2NiTeO_6 containing dark inclusions were grown according to Kohl *et al.* (*7*). Dark red crystals of NiV_2O_6 were grown using excess V_2O_5. Phase identification was by X-ray powder diffraction; cell dimensions of the various compounds refined from Guinier data are included in Table I with crystal growth details.

Oriented single-crystal spectra were measured with calcite polarizers and a Cary 17I spectrophotometer. Spectra of anisotropic crystals were obtained with the vibration direction of the incident light oriented along the principal directions of the refractive index indicatrix (corresponding to the α, β, and γ or ϵ and ω refractive indices). The relationships among optical and crystallographic directions are indicated in the figure captions. Procedures for sample preparation and thickness determination are similar to those previously reported (*8*). For those bands which are superimposed upon a rapidly rising background from the tail of an ultraviolet band, a subjective estimate of the background was subtracted before arriving at ϵ values. All ϵ values are in units of liters per mole-centimeter, calculated per Ni^{2+} ion, where the concentration was calculated using densities obtained via X-ray cell parameters.

Spectra were also obtained from powder samples of $NiWO_4$, $NiNb_2O_6$, $NiTiO_3$, $Ni_3V_2O_8$, and NiV_2O_6. Powder specimens were prepared by solid state reaction. $NiWO_4$ when prepared from $NiCl_2 \cdot H_2O$ and $Na_2WO_4 \cdot 2H_2O$ has a dirty brown color; when prepared from $Ni(OH)_2$ and WO_3, $NiWO_4$ is bright yellow.

The absolute intrinsic absorption coefficients (α, in units of cm^{-1}) of some of the Ni compounds were determined by the dilution method of diffuse reflectance (*9*). Data reduction was based on the assumptions of the Kubelka–Munk theory (*10*). Samples were made by (1) grinding, (2) classifying to remove particles large compared with α^{-1} in spectral regions of interest, and (3) mixing the fines with a large excess of white pigmentary $BaSO_4$ under conditions that prevented agglomeration of colored pigment particles with each other. More details on sample preparation and data analysis have been given elsewhere (*11*). The method permits determination of larger absorption coefficients ($\alpha \geqq 10^4\ cm^{-1}$) than can readily be measured in direct transmission spectroscopy. In this work, the method is used largely for determining the strength and position of the first charge transfer band.

Results

Single-Crystal Spectra

The bulk color of several of the Ni^{2+} materials is determined primarily by the location of the transmission window defined by the wings of the absorption bands in the 800- and 400-nm regions (Figs. 1–13, Table II). For the green compounds,

TABLE I

CRYSTAL GROWTH CONDITIONS AND CELL DIMENSIONS OF Ni^{2+} COMPOUNDS

Product	Starting compositions	Initial temp. (°C)	Holding time (hr)	Final temp. (°C)	Cooling rate (°C/hr)	Appearance, size, cell dimensions
$NiTiO_3$	2.8 g NiO, 3.0 g TiO_2, 51.5 g PbO, 22.2 g V_2O_5	1320	14	950	1	black platelets 0.1 × 5 mm a = 5.0207(5) Å c = 13.785(2) Å
$LiNiPO_4$	4 g LiCl, 4 g Li_3PO_4, 4 g $Ni(OH)_2$, 4 g $NH_4H_2PO_4$	1000	4	300	5	yellow-orange crystals 0.3–0.5 mm a = 10.038(1) Å b = 5.858(1) Å c = 4.680(1) Å
$NiWO_4$	3 g NiO, 10 g WO_3, 53.4 g Na_2WO_4	1250	15	600	2	brown crystals 3–4 mm
$NiNb_2O_6$	6.6 g NiO, 20 g Nb_2O_5, 33 g $Na_4B_2O_7$	1250	8	500	2	yellow-brown crystals 2–3 mm a = 14.034(2) Å b = 5.6821(5) Å c = 5.0220(5) Å
Sr_2NiTeO_6	6.8 g Sr_2NiTeO_6, 117 g $SrCl_2$	1150	24	800	2	yellow-brown crystals 0.3–0.5 mm a = 9.654(3) Å b = 5.613(1) Å c = 5.591(2) Å β = 54.70(2)°
$Li_2Ni_2Mo_3O_{12}$,	2 g NiO 1.8 g Li_2CO_3, 10.8 g MoO_3	1300	8	650	2	yellow-brown crystals ½ × ½ × 2 mm a = 10.410(2) Å b = 17.500(2) Å c = 5.075(1) Å
$Ni_3V_2O_8$	1.611 g NiO, 3.923 g V_2O_5, 4.466 g KVO_3	1000	4	500	10	tan needles 0.1 × 0.2 × 2 mm a = 8.239(1) Å b = 11.387(1) Å c = 5.930(1) Å
NiV_2O_6	1.704 g NiO, 8.296 g V_2O_5	800	4	500	10	dark red transparent platelets 0.1 × 0.2 × 0.3 mm a = 7.130(1) Å b = 8.820(2) Å c = 4.791(5) Å α = 90.15(2)° β = 94.19(2)° γ = 102.15(2)°

the transmission window is centered in the region 510–550 nm (e.g., ~524 nm in NiO and ~540 nm in both $(Mg,Ni)_2SiO_4$ and Ni_2SiO_4). For the bright yellow compounds it is centered in the region 570–580 nm (e.g., ~573 nm in $LiNiPO_4$, 570–580 nm for $MgSiO_3$:Ni, and ~580 nm for $LiScSiO_4$:Ni). For the orange to orange-red compounds it is centered at longer wavelengths (e.g., ~590 nm in $Ni_3V_2O_8$).

TABLE II

ABSORPTION BAND POSITIONS[a]

		Spectral region										
		1400 nm				800 nm			400 nm			
NiO	unpol.			1142			710	643		560	464	415	378
$NiTiO_3$	$\|c$			1330		833	800	745				441	
	$\perp c$			1346		840	798	742				499	
$NiWO_4$	α		1530	1385			819	738			496	438	
	β			1341			837	739		517		443	
	γ			1317			836	739				452	
NiV_2O_6	unpol.			1285			883	767					
$NiNb_2O_6$	α			1363			826	733		508		444	
	β			1428			815	729		506	485	440	
	γ			1333			823	733		509		449	
Ni_2SiO_4	α			1255			788	707		500	474	420	
	β	1482	1372				774	706	621		474	415	376
	γ			1247	1100		786	708			472	423	378
$Ni_3V_2O_8$	α			1270			733						
	β			1277			741						
	γ		1540	1260		843	732			534			
$LiNiPO_4$	α		1620				806	704			473	424	
	β	1775	1450	1304			811	704		504	472	426	
	γ			1297			798	702		512	466	424	
$Li_2Ni_2Mo_3O_{12}$	α			1389			810	732				434	
	β			1303			813	735				440	
	γ			1352			811	738		526		434	
Sr_2NiTeO_6	unpol.		1621	1432			865	732	702	516		461	
$LiScSiO_4$: Ni	α			1367			833	712		522	485	427	
	β		1705	1378			840	714	676			425	
	γ			1330			840	713			487	431	
$MgSiO_3$: Ni	α	2025		1389			804				462	409	
	β	2050		1483				771	670		464	408	
	γ	2050		1540		937		771			464	408	
(Mg, Ni)SiO_4	α			1272			796	708	630	505	479	422	
	β		1435	1299	1104		777	709	644			419	384
	γ			1288	1208		793	709	632		478	425	

[a] In cases where the bands are broad, overlapping, or asymmetric, the tabulated value represents our best estimate of the band maximum. Several very weak, presumably spin-forbidden, bands which are not tabulated above can be observed in the data. All bands are tabulated in units of nm.

The exact wavelength of the transmission maximum will depend on the polarization for the low-symmetry compounds.

Other compounds, such as $NiTiO_3$, Sr_2NiTeO_6, and NiV_2O_6, either do not have a transmission window centered in the visible portion of the spectrum, or it is centered so far into the red that the wings of the long-

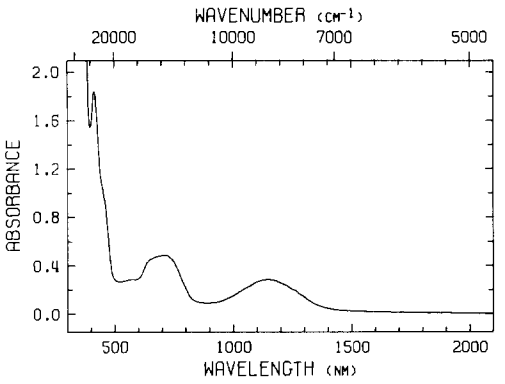

FIG. 1. Absorption spectrum of NiO plotted as 13.3 μm thick.

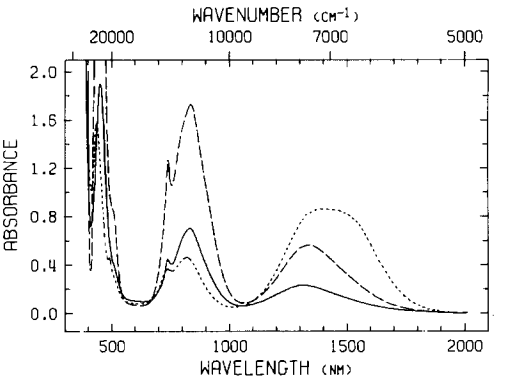

FIG. 3. Absorption spectrum of $NiWO_4$ plotted as 24.0 μm thick. ---, $\alpha \approx c$; ——, $\beta = b$; ——. $\gamma \approx a$; $\alpha \wedge c = 13°$.

wavelength band do not appreciably influence the color. Likewise, the long-wavelength wings of $NiWO_4$, $NiNb_2O_6$, and $Li_2Ni_2Mo_3O_{12}$ are too weak at visible wavelengths to have much influence on color. In these cases, the color is caused predominantly by the tail of the absorption bands centered at less than 400 nm. The net result is a yellow-orange to red color for thin samples. The bulk color of millimeter-sized crystals of several of the compounds with this type of spectrum (e.g., $NiTiO_3$ and NiV_2O_6) is black because of the overall high level of absorption throughout the visible region.

The color of several of the compounds is dependent upon the presence of medium-intensity, low-energy components of the 400-nm region absorption system. These occur at ~464 nm in the $MgSiO_3$: Ni spectra, ~472 and ~512 in the $LiNiPO_4$ spectra, and ~508 nm in the $NiNb_2O_6$ spectra. These components also occur in the spectra of $NiWO_4$, Sr_2NiTeO_6, and $LiScSiO_4$: Ni. In the spectra of several of the compounds, multiple components are found on the long-wavelength side of the primary band near 400 nm. Our estimates of the ϵ values of these bands range from 2.0 for $Li_2Ni_2Mo_3O_{12}$ to 14.1 and 17.3 for $LiNiPO_4$

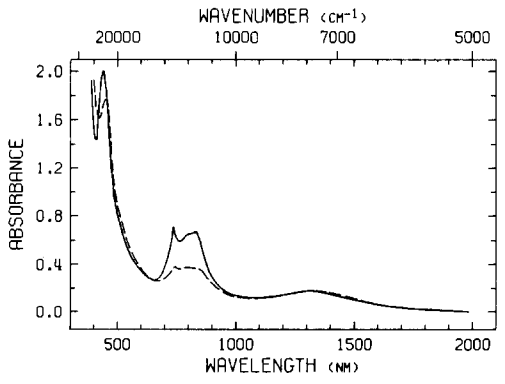

FIG. 2. Absorption spectrum of $NiTiO_3$ plotted as 5.0 μm thick. Solid line, polarized $\|c$; dashed line, polarized $\perp c$.

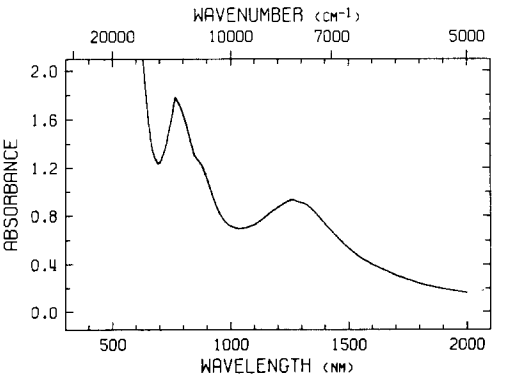

FIG. 4. Absorption spectrum of NiV_2O_6 plotted as 33 μm thick. Unpolarized; orientation of crystal not determined.

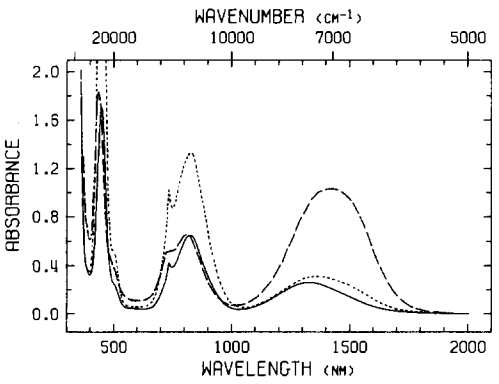

FIG. 5. Absorption spectrum of $NiNb_2O_6$ plotted as 60 μm thick. ---, $\alpha = b$; ——, $\beta = a$; ——, $\gamma = c$.

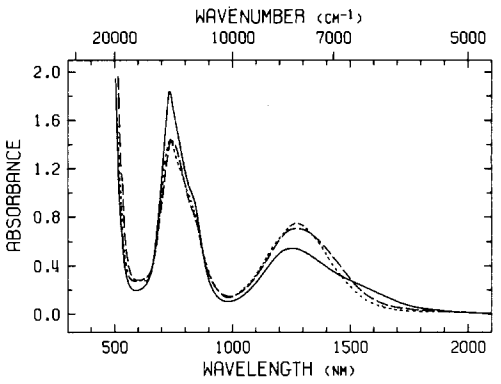

FIG. 7. Absorption spectrum of $Ni_3V_2O_8$ plotted as 40 μm thick. ---, $\alpha = b$; ——, $\beta = c$; ——, $\gamma = a$.

and $MgSiO_3$:Ni, respectively. These last two materials have the brightest yellow color of the substances studied.

Diffuse Reflectance Spectra

Intrinsic absorption spectra obtained from diffuse reflectance for the materials tested are given in Fig. 14. Strong, charge transfer transitions dominate the colors of $Ni_3V_2O_8$ and NiV_2O_6 in the visible. The three compounds with their charge transfer edge in the near uv are listed in Table 4 together with the wavelength at which $\alpha = 10^5$ cm^{-1}. Also shown are suitable averages of the single-crystal ϵ values at ~400 nm. For the uniaxial case, the average is $(2\epsilon_\perp + \epsilon_\parallel)/3$. For biaxial systems the average of the three ϵ values is given. We see that for the three compounds examined, the larger ϵ values are associated with closer proximity to the uv charge transfer transitions.

Accuracy in the dilution method of diffuse reflectance requires that the concentration of colored material in the white diluent be not much larger than 1% and that the reflectance of the mixture lie in the region $0.2 < R < 0.6$. While it is well suited to measurements of absorption coefficients in the range $\alpha > 10^4$ cm^{-1}, the method is not as good for measurements of $\alpha < 10^3$ cm^{-1}, particularly in mixtures designed for measuring the stronger charge transfer transitions. Accordingly, the *d–d* transitions that form the main subject of the paper are only

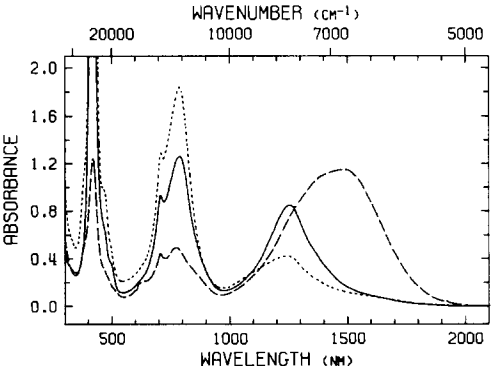

FIG. 6. Absorption spectrum of Ni_2SiO_4 plotted as 35 μm thick. ---, $\alpha = b$; ——, $\beta = c$; ——, $\gamma = a$.

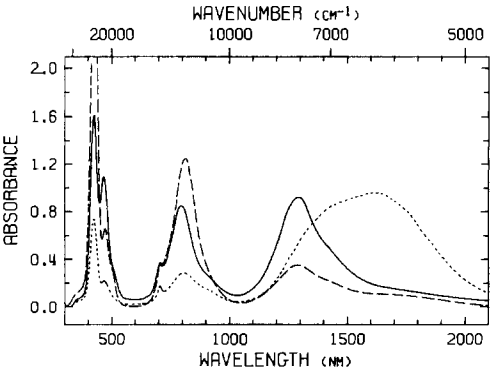

FIG. 8. Absorption spectrum of $LiNiPO_4$ plotted as 30 μm thick. ---, $\alpha = c$; ——, $\beta = a$; ——, $\gamma = b$.

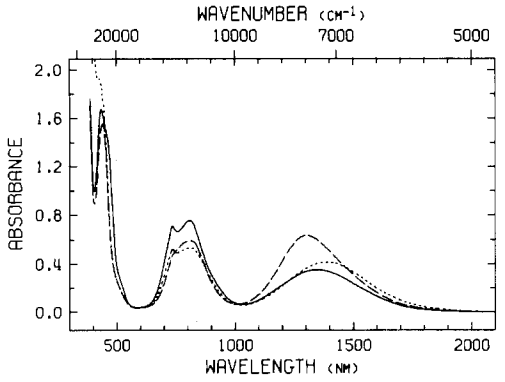

FIG. 9. Absorption spectrum of $Li_2Ni_2Mo_3O_{12}$ plotted as 50 μm thick. – – –, $\alpha = c$; — —, $\beta = a$; ——, $\gamma = b$.

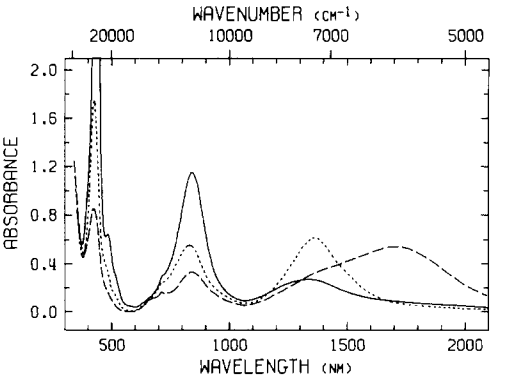

FIG. 11. Absorption spectrum of $LiScSiO_4$: Ni plotted as 360 μm thick. – – –, $\alpha = b$; — —, $\beta = c$; ——, $\gamma = a$.

weakly observable in the diffuse reflectance spectra taken to determine the position of the first charge transfer band. Nevertheless, the relative increase above background observed in the spectra of Fig. 14 near 450 nm is consistent with the relative single-crystal minimum ϵ values there.

Electronic Origin of the Absorption Bands

The general features of Ni^{2+} absorption have been described in terms of ligand field theory. In a rigorously octahedral environment, Ni^{2+} will have three prominent absorption bands, arising from transitions from the $^3A_{2g}$ ground state to the $^3T_{2g}$, $^3T_{1g}(F)$, and $^3T_{1g}(G)$ states. These correspond to the prominent absorption bands in the 1400, 800, and 400-nm regions, respectively (*12*, *13*). Reinen (*14*, *15*) examined the reflection spectra of a variety of compounds with Ni^{2+} in sixfold coordination and concluded that transitions to the singlet states account for the remaining minor features in the spectra. Strong spin–orbit coupling together with antiferromagnetic interactions is believed to increase the intensity of the transition to the ^1E_g state at ~720–740 nm such that it becomes more intense than the spin-allowed transition to the $^3T_{1g}$ state in the case of NiO. Likewise the transition to the $^1T_{1g}$ state at 378 nm is more intense than the 415 nm $^3T_{1g}$ band in NiO.

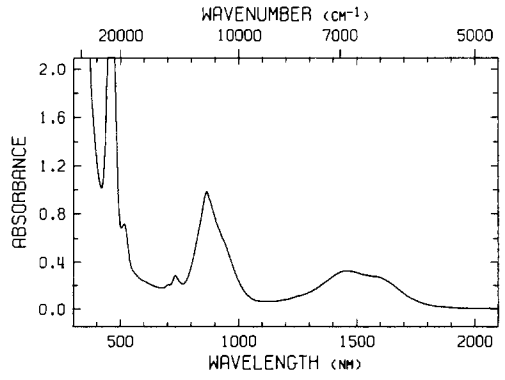

FIG. 10. Absorption spectrum of Sr_2NiTeO_6 plotted as 100 μm thick. Unpolarized.

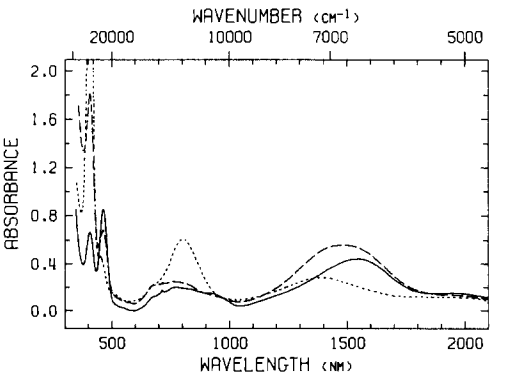

FIG. 12. Absorption spectrum of $MgSiO_3$: Ni plotted as 250 μm thick. – – –, $\alpha = b$; — —, $\beta = a$; ——, $\gamma = c$.

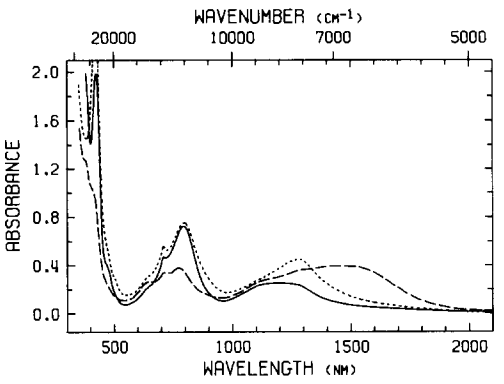

FIG. 13. Absorption spectrum of (Mg, $Ni)_2SiO_4$ plotted as 42 μm thick. ---, $\alpha = a$; ——, $\beta = c$; ——, $\gamma = b$.

Intensities

The greatest absorption band intensities in the 400-nm region are associated with metal ion absorption bands in proximity to an ultraviolet charge transfer tail (e.g., $NiTiO_3$) or with Ni^{2+} in a distorted site (e.g., $MgSiO_3$: Ni). The same effects operate in the 800-nm region, but are not clearly identifiable in the 1400-nm region. The most intense bands, those of $NiTiO_3$, are about an order of magnitude more intense than those of reference Ni^{2+} compounds in aqueous solutions and NiO. Proximity to an ultraviolet charge transfer tail has been recognized to be an important factor in determining the intensities of electronic transitions of metal ions in general through the mechanism of "intensity stealing" (*16*).

The extent to which the ultraviolet charge transfer band extends into the visible region depends in part on the ion with which the Ni^{2+} shares oxygen ions. Easily reduced ions such as V^{5+} and Ti^{4+} produce a charge transfer tail which extends well into the visible region, whereas difficultly reduced ions such as P^{5+} and Si^{4+} do not. Intermediate tails are observed for W^{6+}, Mo^{6+}, and Nb^{5+}. The point at which the absorption on the charge transfer tail rises to 200/cm is included in Table III. The contribution of overlapping Ni^{2+} bands was visually subtracted to obtain these values. [The point at which it rises to 10^5/cm is shown in Table IV.] For systems with charge transfer bands extending over much of the visible region, as $Ni_3V_2O_8$ and NiV_2O_6 (Fig. 14), the color of the material is dominated by the influence of the tail.

Site Symmetry

Site symmetry influences the color of Ni^{2+} compounds. The degeneracy of the $^3T_{1g}$, $^3T_{2g}$, and ^3E_g states of Ni^{2+} in octahedral geometry are lifted and multiple-absorption bands occur when Ni^{2+} is situated in a coordination environment of low symmetry. Bands split by low symmetry will show peak wavelengths which are polarization dependent (*17*). Such splittings are present in the spectra of most of the compounds we studied, and are especially pronounced in the spectra of compounds with the olivine and orthopyroxene structure. The compounds with the brightest yellow color, $LiNiPO_4$ and $MgSiO_3$: Ni, also have the most pronounced splitting of the absorption bands.

Band intensities often increase in response to low site symmetry. The high

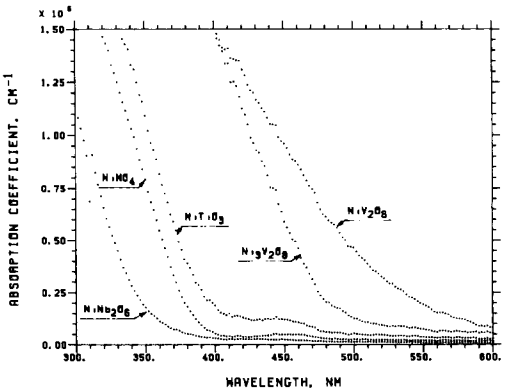

FIG. 14. Absorption spectra of $NiNb_2O_6$, $NiWO_4$, $NiTiO_3$, $Ni_3V_2O_8$, and $NiVO_6$ powders obtained from diffuse reflectance.

TABLE III

ϵ VALUES OF Ni^{2+} COMPOUNDS (liters/mole · cm)

Compound	Polarization	Spectral region[a]			C.T. abs = 200/cm[b] (nm)
		1400 nm	800 nm	400 nm	
NiO	unpol.	2.1	3.7	12.6	390
$NiTiO_3$	$\perp c$	7.5	13	88	600
	$\parallel c$	7.9	32	102	590
$NiWO_4$	α	3.0	9.8	28.4	422
	β	7.9	25.0	46.7	417
	γ	16.5	6.2	22.0	415
NiV_2O_6	unpol.	9.5	20	n.d.	650
$NiNb_2O_6$	α	3.0	12.8	30.9	365
	β	10.0	5.9	17.6	373
	γ	2.5	6.1	16.7	367
Ni_2SiO_4	α	5.0	6.8	21.1	280
	β	6.9	2.5	7.5	280
	γ	2.3	9.9	28.6	280
$Ni_3V_2O_8$	α	7.3	13.8	n.d.	520
	β	6.6	14.0	n.d.	520
	γ	4.9	17.7	n.d.	520
$LiNiPO_4$	α	13.5	3.7	9.9	<300
	β	4.8	17.6	37.1	<300
	γ	12.5	11.5	22.0	<300
$Li_2Ni_2Mo_3O_{12}$	α	6.4	7.8	—	~420
	β	8.6	7.8	21.4	~400
	γ	4.5	9.6	21.5	~400
Sr_2NiTeO_6	unpol.	2.4	7.3	16.9	373
$LiScSiO_4$: Ni	α	5.4	5.0	15.6	310
	β	4.9	3.0	7.7	310
	γ	2.0	9.8	32	310
$MgSiO_3$: Ni	α	5.9	12.5	67	320
	β	11.6	4.7	34	320
	γ	9.0	4.2	10	320
$(Mg, Ni)_2SiO_4$	α	2.8	4.3	14.9	340
	β	3.0	2.6	2.4	390
	γ	1.7	5.0	18.1	410

Note. n.d. = not determined.

[a] The ϵ values under these headings refer to the intensity of the most intense band in the region near 1400, 800, and 400 nm. They are computed disregarding multiple-site occupancy of nickel.

[b] The wavelength at which the ultraviolet charge transfer tail reaches an absorbance of 200/cm of crystal thickness.

intensities of the $LiNiPO_4$ absorptions are an example. The high intensity of the 457-nm spin-forbidden band of Ni^{2+} clinopyroxene previously noted by White *et al.* (*18*) is analogous to the intensity of the 464-nm band in $MgSiO_3$: Ni.

TABLE IV

ϵ VALUES AT 400 nm COMPARED WITH POSITION OF CHARGE TRANSFER BAND

	ϵ at 400 nm (l mole^{-1} cm^{-1})	$\alpha = 10^5$ cm^{-1} (nm)
$NiTiO_3$	92.7	352
$NiWO_4$	32.4	340
$NiNb_2O_6$	21.7	305

Correlations

Correlations were examined between structural, ligand field, and other spectroscopic parameters. In general, no strong correlations were established. For Ni^{2+} in a rigorously octahedral site, the value of the ligand field parameter Dq is equal to 1/10th the energy of the transition to the lowest energy $^3T_{2g}$ state. In a site of low symmetry, the transition to $^3T_{2g}$ is split into up to three components. We defined $10Dq$ to be equal to the average of the transition energies of the three components in the 1400-nm region.[1] In some cases our values differ from those obtained from diffuse reflectance spectra because we have included weak, low-energy components which were not identified in previous studies. Faye had presented a linear correlation between the average Ni–O distance and Dq for a series of compounds containing six-coordinated Ni^{2+} (*19*). Unfortunately, this correlation fails for $NiWO_4$, $NiTiO_3$, $Ni_3V_2O_8$, $NiNb_2O_6$, Sr_2NiTeO_6, and $Li_2Ni_2Mo_3O_{12}$. Likewise, Dq does not correlate with a parameter which measures the distortion of the Ni^{2+} site defined by:

$$\text{Distortion Parameter} = \tfrac{1}{6}\Sigma\{(R_i - \bar{R})/\bar{R}\}^2,$$

where $\bar{R}$ is the mean Ni–O distance and R_i's are the individual Ni–O distances. Furthermore, Dq does not correlate well with the ϵ values. Determination of ligand field parameters is complicated by multiple-site occupancy in some compounds. In Ni_2SiO_4, for example, Ni^{2+} occurs in two sites, $M1$ and $M2$, which are crystallographically distinct. (*20*). The overlapping contributions from Ni^{2+} in both sites are present in the spectrum. The overlap of bands from multiple sites and low site symmetry both render detailed calculation of ligand field parameters impractical.

[1] For biaxial crystals $10Dq = \frac{1}{3}[E(\alpha) + E(\beta) + E(\gamma)]$. For uniaxial $NiTiO_3$ $10Dq = \frac{1}{3}[2E(\perp c) + E(\parallel c)]$.

Comparison to Other Studies

The details of intensities and band shapes of the NiO single-crystal spectra are different from that of $MgO:Ni^{2+}$ crystal data (*12, 21*), particularly with regard to the presence of the 560-nm band, which was also observed in NiO by Newman and Chrenko (*22*). Most previous studies of nickel compounds have been by reflection spectroscopy. We frequently find differences in both band positions and relative intensities between the single-crystal data and those calculated from reflectance data on concentrated powers. These studies include: $NiTiO_3$ (*14*), Ni_2SiO_4 (*23, 24*), and $(Mg,Ni)_2SiO_4$ (*23*). Overall good agreement was observed between our Sr_2NiTeO_6 single-crystal data and the reflectance data of Kohl (*25*). Spectroscopic crystal field parameters only have been reported for $NiNb_2O_6$ (*15*). White *et al.* (*18*) concluded that Ni^{2+} was situated on the larger, distorted $M2$ site of the yellow, monoclinic pyroxene $MgSiO_3:Ni$. Their conclusion was based on the small value of Dq and the large value of the Racah parameter B. Similar values of these parameters are calculated from our $MgSiO_3:Ni$ spectrum. The low energy components near 2000 nm indicate greater than usual splitting of the lowest $^3T_{1g}$ state and are further evidences for the occupancy by Ni^{2+} of the distorted $M2$ site.

Reinen (*23*) concluded from reflectance

spectra that although Ni^{2+} preferentially orders on $M1$ in $(Mg,Ni)_2SiO_4$, low-energy components on the three primary band systems were from Ni^{2+} in the $M2$ site. In the spectrum of Ni_2SiO_4, Wood (*24*) identified contributions from both the $M1$ and $M2$ sites; however, our single-crystal spectra differ significantly from his fit of a reflectance spectrum.

Conclusions

Bright yellow Ni^{2+} compounds can occur as a consequence of nickel entering six-coordinated sites significantly distorted from octahedral geometry. The color is a result of electronic transitions localized on the Ni^{2+}. Yellow compounds also result from intense charge transfer tails centered in the ultraviolet. These are associated with easily reduced cations. Higher absorption coefficients are associated with proximity to uv charge transfer bands through the mechanism of "intensity stealing."

Acknowledgments

Jun Ito, University of Chicago, provided the nickel silicates and their chemical analyses for this study. Jeff Hare and Don S. Goldman assisted with some of the optical measurements. We also acknowledge B. F. Gordon for sample preparation, C. M. Foris and E. P. Moore for assistance in X-ray diffraction, and J. J. O'Reilly for assistance in the diffuse reflectance measurements.

References

1. I. N. Steele, J. J. Pluth, and J. Ito, *Z. Kristallogr.* **147,** 119 (1978).
2. F. C. Hawthorne and J. Ito, *Canad. Mineral.* **15,** 321 (1977).
3. G. Garton, S. H. Smith, and B. M. Wanklyn, *J. Crystal Growth* **13,** 588 (1972).
4. F. Zambonini and L. Malossi, *Z. Kristallogr.* **80,** 442 (1931).
5. B. M. Wanklyn, *J. Mater. Sci.* **7,** 813 (1972).
6. B. M. Wanklyn, F. R. Wondre, and W. Davison, *J. Mater. Sci.* **11,** 1607 (1976).
7. P. Kohl, E. Schultze-Rhonhof, and D. Reinen, *Z. Anorg. Allg. Chem.* **378,** 129 (1970).
8. G. R. Rossman, *Amer. Mineral.* **60,** 698 (1975).
9. G. Kortum, "Reflectance Spectroscopy," p. 175. Springer-Verlag, New York (1969).
10. G. Kortum, "Reflectance Spectroscopy," p. 106. Springer-Verlag, New York (1969).
11. R. K. Waring, "NBS Special Publication," Vol. **574,** p. 152. National Bureau of Standards, Washington, D.C. (1980).
12. W. Low, *Phys. Rev.* **109,** 247 (1958).
13. A. D. Liehr and C. J. Ballhausen, *Ann. Phys.* **6,** 134 (1959).
14. D. Reinen, *Ber. Bunsenges.* **69,** 82 (1965).
15. D. Reinen, *Theor. Chim. Acta (Berlin)* **5,** 312 (1966).
16. R. F. Fenske, *J. Amer. Chem. Soc.* **89,** 252 (1967).
17. A. B. P. Lever, G. London, and P. J. McCarthy, *Canad. J. Chem.* **55,** 3172 (1977).
18. W. B. White, G. J. McCarthy, and B. E. Scheetz, *Amer. Mineral.* **56,** 72 (1971).
19. G. H. Faye, *Canad. Mineral.* **12,** 384 (1974).
20. G. A. Lager and E. P. Meagher, *Amer. Mineral.* **63,** 365 (1978).
21. R. Pappalardo, D. L. Wood, and R. C. Linares, *J. Chem. Phys.* **35,** 1460 (1961).
22. R. Newman and R. M. Chrenko, *Phys. Rev.* **114,** 1507 (1959).
23. D. Reinen, *Z. Anorg. Chem.* **356,** 182 (1968).
24. B. J. Wood, *Amer. Mineral.* **59,** 244 (1974).
25. P. Kohl, *Z. Anorg. Allg. Chem.* **427,** 205 (1976).